



HAL
open science

Highly efficient few-mode spatial beam self-cleaning at $1.5\mu\text{m}$

Yann Leventoux, A. Parriaux, O. Sidelnikov, Geoffroy Granger, Mathieu Jossent, Laure Lavoute, D Gaponov, Fabert Marc, Alessandro Tonello, katarzyna Krupa, et al.

► **To cite this version:**

Yann Leventoux, A. Parriaux, O. Sidelnikov, Geoffroy Granger, Mathieu Jossent, et al.. Highly efficient few-mode spatial beam self-cleaning at $1.5\mu\text{m}$. Optics Express, 2020, 28 (10), pp.14333-14344. 10.1364/OE.392081 . hal-03426175

HAL Id: hal-03426175

<https://hal.science/hal-03426175>

Submitted on 12 Nov 2021

HAL is a multi-disciplinary open access archive for the deposit and dissemination of scientific research documents, whether they are published or not. The documents may come from teaching and research institutions in France or abroad, or from public or private research centers.

L'archive ouverte pluridisciplinaire **HAL**, est destinée au dépôt et à la diffusion de documents scientifiques de niveau recherche, publiés ou non, émanant des établissements d'enseignement et de recherche français ou étrangers, des laboratoires publics ou privés.

Highly efficient few-mode spatial beam self-cleaning at 1.5 μ m

Y. LEVENTOUX,¹ A. PARRIAUX,² O. SIDELNIKOV,³ G. GRANGER,¹ M. JOSSENT,⁴ L. LAVOUTE,⁴ D. GAPONOV,⁴ M. FABERT,¹ A. TONELLO,¹ K. KRUPA,⁵ A. DESFARGES-BERTHELEMOT,¹ V. KERMENE,¹ G. MILLOT,^{2,6} S. FÉVRIER,¹ S. WABNITZ,^{3,7} AND V. COUDERC^{1,*}

¹Université de Limoges, XLIM, UMR CNRS 7252, 123 Av. A. Thomas, 87060 Limoges, France

²Université de Bourgogne Franche-Comté, ICB, UMR CNRS 6303, 9 Av. A. Savary, 21078 Dijon, France

³Novosibirsk state University, Ulitsa Pirogova, 2, Novosibirskaya oblast' 630090, Russia

⁴Novae, ZI du Moulin Cheyoux, 87700 Aix sur Vienne, France

⁵Institute of Physical Chemistry Polish Academy of Sciences, ul. Kasprzaka 44/52, 01-224 Warsaw, Poland

⁶Institut Universitaire de France (IUF), 1 rue Descartes, Paris, France

⁷Dipartimento di Ingegneria dell'Informazione, Elettronica e Telecomunicazioni, Sapienza University of Rome, Via Eudossiana 18, 00184 Rome, Italy

Abstract: We experimentally demonstrate that spatial beam self-cleaning can be highly efficient when obtained with a few-mode excitation in graded-index multimode optical fibers. By using 160 ps long, highly chirped (6 nm bandwidth at -3dB) optical pulses at 1562 nm, we demonstrate a one-decade reduction of the power threshold for spatial beam self-cleaning, with respect to previous experiments using pulses with laser wavelengths at 1030-1064 nm. Self-cleaned beams remain spatio-temporally stable for more than a decade of their peak power variation. The impact of input pulse temporal duration is also studied.

1. Introduction

Nonlinear beam propagation in multimode optical fibers (MMFs) is currently being extensively investigated as a test-bed of fundamental wave propagation effects, and for a variety of different applications [1]. These include: increasing the capacity of future long-distance communications using spatial division multiplexing [2], nonlinear microscopy and endoscopy [3], and scaling up the energy of fiber laser sources [4,5], to name a few. In applications where MMFs are used for beam delivery, an important problem to be solved is the effective coupling and stable transport of a diffraction limited optical beam from a single mode (SM) laser source into the fundamental mode of the MMF. Random mode coupling may limit the MMF length to a few tens of cm, before the beam quality is severely degraded. Although in MMF amplifiers, an effective SM propagation can be achieved by gain-guiding [6], in passive graded-index (GRIN) MMFs spatial beam self-cleaning towards the fundamental, as well as different low-order modes, has been demonstrated in the normal group velocity dispersion (GVD) regime, by exploiting the intensity-dependent refractive index of the fiber [7–13]. Recent studies by E. V. Podivilov et al. [14] and A. Fusaro et al. [15] pointed out the interesting links between beam self-cleaning and the wave condensation phenomenon, that is predicted by 2D hydrodynamic wave turbulence, or classical wave thermalization [16], respectively. On the one hand, the theory of beam condensation in a multimode GRIN fiber predicts that, asymptotically, the fraction of power coupled into the fundamental mode increases by reducing the number of modes that are initially excited at the fiber input [16]. In particular, the theory developed in Ref. [15] pointed out that longitudinal disorder (or random linear mode coupling) induces a significant acceleration of the rate of condensation, which may permit a better matching between observations of the self-cleaning effect, and wave condensation theory. As a matter of fact, an experimental validation of the condensation theory was carried out, by controlling the wave front launched into a GRIN MMF with a diffuser. This permits to change the number of excited modes, while keeping constant the input power [15]. On the other hand, a recent theoretical study has predicted that, whenever a small number of modes is coherently excited at the input of a short length of GRIN MMF, the processes of thermalization and condensation are virtually inhibited [17]. Therefore, the important question arises: is it still possible to observe a beam self-cleaning effect under few-mode excitation conditions, and for what input threshold powers? To answer this question, we experimentally investigate the process of beam self-cleaning in GRIN-MMFs under the condition of few-mode coherent excitation. We obtained this condition by using a laser pump at 1562 nm, that is, within the telecom spectral window. We used an input beam from a SM fiber laser source, as it was done in previous experiments for generating multimode fiber solitons (MMSs) [18]. However, instead of femtosecond input pulses, we used long (160 ps), pre-chirped optical pulses. The use of such long pulses permits to neglect both modal and chromatic dispersion effects in their propagation over ~ 10 m of GRIN MMF. Still, as we shall see, previously unforeseen, and highly efficient, spatiotemporal nonlinear attractors emerge from nonlinear multimode propagation in the MMF. We found that the pulse at the fiber output exhibits a very robust spatial reshaping into the fundamental LP₀₁ mode. Moreover, depending on the specific input spatial coupling conditions (*i.e.*, the incidence angle of the beam), a beam self-cleaning in the odd low-order LP₁₁ mode can also be obtained at the fiber output. This effect, as we shall explain later in the

text, may be interpreted as the generation of transient beam, before its eventual decay into the fundamental mode at longer distances. The optimized, and nearly SM excitation conditions lead to highly efficient spatial beam self-cleaning. Namely, the power threshold for self-cleaning is reduced by one order of magnitude with respect to previous experiments carried out in the normal GVD regime, and based on highly multimode excitation.

2. Preliminary analysis

2.1. Influence of pulse duration with large number of initially excited modes at 1064nm

In purely spatial beam self-cleaning experiments, the temporal duration of the laser pulses must be sufficiently long, in order to neglect linear dispersive effects (differential group delay (DGD) and GVD) over the involved fiber length. In a first series of experiments, we studied the influence of input pulse duration on the stability of beam self-cleaning with respect to input power variations. For input powers above a certain threshold value, self-cleaning leads to a bell-shaped beam, close to the fundamental mode, at the output of a GRIN MMF [1,8].

We used various laser sources delivering Fourier transform-limited pulses with different temporal durations at 1064 nm (normal dispersion regime for the MMF). The Gaussian pump beam diameter at the input fiber face is 36 μm (measured at $1/e^2$), corresponding to the excitation of more than 18 transverse modes for all experiments shown in Fig. 1 (50/125 GRIN-MMF). For input peak powers above a threshold value, self-cleaning in a 3-m long GRIN MMF leads, first, to energy transfer into the fundamental mode, followed, in a second step, by self-phase modulation [8]. In Fig. 1, we display a series of spectrograms showing, in the vertical coordinate, the x-transverse dimension of the output beam intensity from the GRIN MMF. Whereas the horizontal dimension indicates the corresponding pulse spectrum (vs. wavelength). In each row, the input pulse power increases from left to right. The leftmost column refers to the case of linear pulse propagation: the beam size is wide, owing to the speckled output. In the middle column, we show the case corresponding to the power threshold for self-cleaning (here 1 kW). As can be seen, the beam size is spatially compressed down to the size of the fundamental mode of the MMF, while the spectrum remains nearly as narrow as in the linear regime. This shows that at the beam self-cleaning threshold, self-phase-modulation (SPM) induced spectral broadening remains negligible. Finally, the rightmost column corresponds to the high-power regime, where SPM leads to significant spectral broadening.

In the top row of Fig. 1, the input pulse duration was $\tau = 740$ ps, which is about 61 times longer than the DGD in the MMF, owing to intermodal group velocity dispersion. In the bottom row, on the other hand, the input pulse duration was reduced down to $\tau = 6$ ps, that is nearly equal to the fiber DGD. The middle row corresponds to the intermediate case with $\tau = 60$ ps, or five times the DGD. As can be seen in Fig. 1, beam self-cleaning remains stable (with respect to large variations of the input peak power), in spite of the addition of SPM, only in the case of a pulse whose duration is much longer than the DGD, or in the quasi-continuous wave regime, which was recently studied by Krupa et al. [7,8,11]. Therefore, we confirmed experimentally that in order to observe beam self-cleaning, it is necessary that the corresponding power threshold remains, lower than the power level where one observes significant SPM-induced spectral broadening. At the same time, the input pulse duration must be much longer than the fiber DGD. Although the results of Fig. 1 were obtained with laser sources emitting at 1064 nm, thus in the normal GVD regime of the MMF, the generality of these conclusions does not depend on the sign of chromatic dispersion (for fiber lengths much shorter than the chromatic dispersion length).

2.2. Impact of the number of initially excited modes with sub-ns long pulses at 1064 nm

Now, the possibility of observing spatial beam self-cleaning also in situations involving a small number of initially excited modes is crucial for practical applications, where the main goal is to obtain a highly efficient nonlinear beam reshaping process, with the lowest possible input power threshold value. The impact of the input beam diameter, and its consequences on the polarization state beam self-cleaning was already explored in Ref. [19].

Therefore, in a second series of experiments we studied the impact of the number of excited modes on the properties of the self-cleaning process. We used sub-ns long pulses at 1064 nm that, in contrast to previous experiments [15–16], we injected into the GRIN MMF by imposing a transverse shift to the lateral position of the Gaussian beam with respect to the fiber core, while keeping the guided peak power fixed. We recorded the output beam intensity pattern both in the linear and nonlinear regimes (see Fig. 2). As can be clearly seen, the excitation of the MMF at the exact central position minimizes the energy coupled into high-order modes which permits, at the same time, to rapidly reach the beam cleaning power threshold (at 40 kW input peak power) over three meters of fiber only. Conversely, the larger the transverse shift of the input beam x , the higher the number of excited modes, and the higher is the power threshold for beam cleaning.

A different method to decrease the number of excited modes, hence to obtain highly efficient beam cleaning with a relatively low power threshold, involves an increase of the input beam wavelength. Indeed, as confirmed by our numerical simulations, presented in Fig. 3, while keeping fixed the diameter of the beam spot at the fiber input, it is possible to decrease the number of excited modes by simply increasing the beam wavelength.

2.3. Excitation of a few low-order modes with long chirped pulses at 1562 nm

In a third and final series of experiments, presented in the next section of the paper, we studied the possibility to achieve highly efficient self-cleaning by exploiting our previous results. We used a laser delivering relatively long (160 ps), pre-chirped optical pulses at 1562 nm. In this configuration, and by limiting our maximum peak power to levels of the order of 1 kW, we can simultaneously mitigate the effects of SPM-induced spectral broadening, GVD and DGD.

Moreover, our initial beam leads to the initial population of just a few, low-order GRIN fiber modes.

3. Experiments

3.1. Experimental set-up

Our set-up to observe beam self-cleaning at telecom wavelengths was based on dispersive broadening (and chirping) of the full-width at half maximum (FWHM) duration fiber laser pulses from 1 ps to 160 ps. The spectral bandwidth at -3 dB of input pulses was 6 nm. The center of the fiber laser wavelength was 1562 nm, with 1 MHz repetition rate. The laser beam was coupled into a 12 m long piece of GRIN MMF by means of a short section of standard single mode fiber (SSMF). As a consequence, as in Ref.[18], the initial spatial beam profile is provided by the fundamental mode of the SSMF, with a mode field diameter of 11.5 μm (measured at $1/e^2$). This leads to optimized free-space coupling efficiency (up to 80%) into the GRIN MMF. The GRIN MMF of 12 m length was loosely coiled on the table forming rings of ~ 15 cm diameter. The fiber had a circular core of 25 μm radius, with a core-cladding index difference of 0.015, corresponding to a 0.2 numerical aperture. We numerically estimated that these input conditions lead to more than 99% of the guided input power coupled into the first three-four radial symmetry modes only (see Fig. 3). The diameter and low number of spots in the linear output beam pattern (see panels for 3-6 W input peak powers in Fig. 4) is also a direct signature of energy coupling into a small number of modes. As we shall see, few-mode excitation greatly facilitates the output beam cleaning process, and leads to greatly reduced input power thresholds with respect to experiments carried out at 1064 nm, with much larger relative input beam diameters (Fig. 2). Moreover, Fig. 3 shows that the use of a longer wavelength (i.e., 1562 nm versus 1064 nm), while keeping the initial beam diameter fixed, allows for the excitation of a reduced number of modes in the GRIN fiber, which should also favor the self-cleaning process. It is important to recall that, for the practical use of self-cleaning as a means to achieve high-power beam delivery using GRIN fibers, the input beam diameter leading to optimized coupling efficiency should always be chosen. Now, this optimized diameter is about 36 μm at 1064 nm (leading to many-mode excitation, and relatively high self-cleaning power threshold), while it reduces down to about 11.5 μm at 1562 nm (leading to few-mode excitation, and reduced power threshold).

3.2. Self-cleaning on fundamental mode

Figure 4 shows the observed progressive self-cleaning, as the input peak power grows larger, of the output near-field intensity patterns. As can be seen, the speckled output intensity pattern resulting from the coherent superposition of modes at a peak power of about 3W, self-cleans into a bell-shaped beam, with negligible multimode field background, as the peak power grows higher than ~ 100 W. We show in Fig. 5 (solid curve) the intensity correlation C_S of the experimental near field pattern of the output beam with the mode LP₀₁, numerically obtained with a mode solver:

$$C_S = \frac{\int I_{\text{exp}} I_{\text{th}} dS}{\sqrt{\int I_{\text{exp}}^2 dS \int I_{\text{th}}^2 dS}} \quad (1)$$

where I_{exp} and I_{th} represent the experimental output intensity profile and the numerically calculated mode profile, respectively, and the integration is carried out along the fiber cross section S . The intensity correlation C_S with the fundamental mode keeps monotonically increasing as the input peak power grows larger, until reaching more than 95% at high powers. Additionally, far and near field measurements of the output self-cleaned beam allow us to demonstrate that the beam divergence is only 1.15 times higher than that obtained for a pure Gaussian beam.

Figures 4 and 5 show that the process of chirped pulse self-cleaning in our present experiments is much more efficient than in previous experiments carried out at 1064 nm, in two respects.

First, the threshold for self-cleaning is reduced by about one order of magnitude (from 1 kW [8] down to 100 W) for a GRIN fiber length of about 12 m. Second, nearly complete intensity correlation with the fundamental mode is achieved at the fiber output, in contrast with experiments in the normal GVD regime and with a wider input beam, where large residual high-order mode background was generally observed around the self-cleaned beam [8,11], in agreement with the predictions of thermalization and condensation of classical optical waves [16], as well as of the 2D hydrodynamic turbulence model [15].

3.3. Self-cleaning on LP₁₁ mode

In our experiments, by varying the horizontal tilt of the Gaussian laser beam launched at the GRIN-MMF input face, we could also observe the progressive self-selection of the LP₁₁ mode at the fiber output (see Fig. 6). The incident beam intercepted the fiber axis with an angle of 2.5° in order to exit the numerical aperture of the fundamental mode. In this case, the coupled power mainly feeds odd modes, and self-selection was observed above a peak power threshold of about 500 W. Still, the input peak power threshold was about one order of magnitude lower than that for LP₁₁ mode self-selection in the normal GVD regime [12].

Even more remarkable is the high intensity correlation with the LP₁₁ mode, reaching more than 80% at high powers, as illustrated by the green curve of Fig. 5. It is important to underline that the excitation of odd low-order modes first introduces a transfer of the energy towards the LP₁₁ mode. Kerr cleanup into the LP₁₁ mode may be interpreted as a transient effect, that is observed when using with a fiber length shorter than the length required to obtain the eventual cleanup into the LP₀₁ mode [12]. However, in practice, additional unavoidable effects like SPM-induced spectral broadening and Raman scattering, could hamper the experimental observation of the beam relaxation into the fundamental mode. Moreover, as discussed in Ref. [8], SPM leads to a symmetry breaking in parametric mode mixing. Note also that the theory of classical wave condensation [16] does not currently take into account the flow of disorder (entropy) in the time domain, which has been observed [11], and proposed as a mechanism for spatial beam self-cleaning [20].

3.4. Spectral analysis

Besides the stability of the output spatial patterns, the observed nonlinear beam attractor also exhibits a remarkable stability, versus pulse power, in the frequency domain. Figure 7 shows the dependence upon the peak power of the spectral density of pulses attracted into the LP₀₁ mode. As can be seen, the output pulse spectrum remains nearly unchanged, in spite of more than two decades of variation of the input power. SPM-induced spectral broadening only takes place for input powers above 1 kW, that is well above the self-cleaning threshold. The self-cleaning of chirped ultrashort optical pulses is thus analogous to chirped pulse amplification in nonlinear amplifiers [21]: in both cases, the effects of SPM can be reduced by means of pre-chirping the pulses. Although being a weak effect, in our case, the presence of a nonlinear phase shift between the fundamental mode and high-order modes is still required, in order to suppress random mode coupling, and stably maintain beam cleanup.

3.5. Temporal analysis

Figure 8 illustrates the evolution of the output temporal waveforms obtained for self-cleaning on the LP₀₁ mode at different input peak powers, by using a fast photodiode and oscilloscope (temporal resolution 12 ps). The active area of the photodiode was placed at the center of the near-field image of the output beam. The diameter of the active window of the photodiode would appear of only about 4 μm, if one rescales the magnified image of the near field into the 50 μm diameter of the fiber core (for details, see [11]). Thus, the photodiode mainly detects light carried by the fundamental mode. Recall that chromatic and modal dispersion have negligible influence on the output pulse duration.

As can be seen, limited temporal reshaping of the output pulse profile is only observed well above the Kerr cleaning threshold. The envelope profile undergoes temporal modulations, owing to power exchange between transverse modes. This envelope reshaping is similar to that previously reported in the normal dispersion regime with a pump at 1064 nm [11]. In our case, the low number of excited modes, coupled with a relatively long pulse duration at 1562 nm, significantly reduces the observed spatiotemporal reshaping, owing to the limited energy involved in the nonlinear transfer among different modes. However, high-quality output beams are obtained, with angular divergence very close to that obtained for a pure Gaussian beam in the case of an axial MMF excitation.

4. Simulations

To explore the impact of wavelength and input diameter, we carried out numerical simulations with a vector beam propagation method that includes diffraction, dispersion, graded index waveguide, self and cross-phase modulation. The fiber core diameter is 52 μm, the core index is 1.47 and the cladding index 1.457. The group velocity dispersion is assumed constant, and its values are 16.55×10^{-27} s²/m at 1064

nm and $-27.97 \times 10^{-27} \text{ s}^2/\text{m}$ at 1550 nm, respectively. The nonlinear coefficient $n_2=2.62 \times 10^{-20} \text{ m}^2/\text{W}$ in the absence of the Raman effect. Moreover, the fiber disorder is also implemented with a coarse step integration method (see also the results of Ref. [12]), by chaining randomly oriented fiber segments of slightly different ellipticity. The coarse step method is applied every 5 mm: the fiber core is assumed to be slightly elliptical, with lengths of both axes uniformly random distributed in the range of $\sim 0.1 \mu\text{m}$. The orientation angle of each fiber segment is also a uniformly distributed random variable. As a result, speckles are gradually generated along the course of the propagation, when starting from an input purely Gaussian beam.

Note that in all considered cases we used the same sequence of random orientations, so to draw a fair comparison among the different input conditions.

Figure 9 summarizes a series of numerical simulations at either low and high peak powers, with two different sample diameters (measured at FWHM) of 25 μm and 40 μm , respectively and the input pulse duration of 5 ps. The result of the propagation in 1.9 m of fiber of the input Gaussian beam is then a speckled pattern as shown in both panels (a) and (c), when assuming a laser central wavelength of 1064 nm. Note that in the panels of Fig. 9 we report the peak intensity of the input beam, I . The lowest diameter of 25 μm has a peak intensity increased by

a factor $(40/25)^2=2.56$, so that we may compare cases with the same input power. Panels (e) and (f) describe the beam intensity output when the laser wavelength is at 1550 nm: the longer wavelength generates bigger and smoother speckles. We considered input power levels where nonlinear beam shaping was clearly noticeable. Panels (b) and (d) show output patterns at 1064 nm: as can be seen, panel (b) presents a better beam quality than panel (d). This means that, for the same input power, the beam having a smaller initial diameter leads to improved self-cleaning. A similar situation is also seen at 1550 nm, if we compare the result of panel (f) with that of panel (h): once again, for a given input power, a better (i.e., closer to bell-shaped) output beam is obtained when the input diameter is smaller.

5. Discussion and conclusions

To summarize, we have experimentally shown that Kerr-induced beam cleanup in GRIN-MMFs may occur with extreme efficiency when exploiting the regime of few-mode coherent excitation at 1.5 μm . By controlling the input coupling conditions, nearly full reshaping into the fundamental LP_{01} mode has been observed. The selective excitation of asymmetric low-order modes favors instead an initial convergence towards the LP_{11} mode of the MMF. The power threshold for beam self-cleaning on the fundamental mode is reduced by about one order of magnitude, down to about 100 W, with respect to previous experiments at shorter wavelength of $\sim 1 \mu\text{m}$. This significant improvement of the beam cleaning efficiency is due to the input beam conditions, which allowed to coherently excite a low number of transverse modes.

We underline that the particular dispersion regime is not a key parameter here, as long as the pulse is sufficiently long and the initial peak power remains sufficiently low, in order to avoid additional nonlinear effects (such as modulation instability or soliton generation). Note that few-mode excitation at 1 μm (with appropriate beam size), would not be as efficient: as we explained in Section 3.1, such a beam size would not lead to optimized coupling efficiency into the GRIN MMF. Therefore, a higher laser power should be used.

Self-cleaned beams remain nearly unchanged in the frequency domain, for over two decades of variation of the output power, whereas the pulse envelope undergoes a moderate reshaping due to energy exchange between modes. Therefore, if so needed, the pulse, in principle, could be subsequently re-compressed to its original duration by a second dispersive element after that self-cleaning has occurred.

Efficient and stable beam self-cleaning in the fundamental mode of the GRIN fiber is obtained for on-axis excitation, for an input beam size corresponding to optimized coupling efficiency, and it is perfectly suited to the Gaussian beam shape of most laser sources. These are the usual conditions for efficient coupling of light into a GRIN MMF even in linear propagation conditions.

Thus, beam cleaning is well-suited to practical applications, as it has been recently demonstrated for improving the resolution of optoacoustic endoscopy [22], and the beam quality in a multimode mode-locked fiber laser [23]. On the other hand, beam cleaning into other low-order modes requires a careful selection of the incident angle: for practical applications, an adaptive wavefront shaping procedure should be employed [13].

In the presented proof-of-principle demonstration of efficient spatial beam self-cleaning, a GRIN optical fiber with a fundamental mode size close to that of a standard SM fiber was used, so that the SM and the MMF have a comparable power-carrying capability. This does not limit the power scalability of self-cleaned beam delivery: GRIN fibers exist with very large diameters up to 600 μm (and larger fiber diameters can be drawn, if needed). Thus, the fundamental mode of GRIN fibers can reach a diameter

of more than 120 μm , which opens new potentialities for high-power delivery. In addition, the design of new optical fibers with a supergaussian index profile can relax the constraints on the fundamental mode area, while keeping the good efficiency of the Kerr self-cleaning effect [24].

The reported results are relevant for a better understanding of the spatial beam self-cleaning process, and broaden our capabilities to control this particular nonlinear reshaping mechanism, in order to reach highly efficient spatial mode selection. Several applications, such as three-photon imaging in medical microscopy and endoscopy, high-power laser beam delivery for metal cutting and welding, mode-locked multimode fiber lasers and amplifiers operating in the near-infrared, and space-division-multiplexed transmissions with GRIN fibers could benefit from this new spatiotemporal self-reshaping phenomenon.

Funding

H2020 European Research Council (740355); H2020 Marie Skłodowska-Curie Actions (713694); Agence Nationale de la Recherche (ANR-10-LABX-0074-01, ANR-15-IDEX-0003, ANR-16-CE08-0031, ANR-18-CE080016-01); Région Nouvelle Aquitaine (FLOWA); Direction Générale de l'Armement; iXcore; CILAS (X-LAS); Ministry of Education and Science of the Russian Federation (14.Y26.31.0017).

Acknowledgments

We acknowledge helpful discussions with Alain Barthélémy, Adrien Fusaro, and Antonio Picozzi.

Disclosures

The authors declare no conflicts of interest.

References

1. K. Krupa, A. Tonello, A. Barthélémy, T. Mansuryan, V. Couderc, G. Millot, P. Grelu, D. Modotto, S. A. Babin, and S. Wabnitz, "Multimode nonlinear fiber optics, a spatiotemporal avenue," *APL Photonics* **4**(11), 110901 (2019).
2. S. Mumtaz, R. J. Essiambre, and G. P. Agrawal, "Nonlinear propagation in multimode and multicolor fibers: generalization of the Manakov equation," *J. Lightwave Technol.* **31**(3), 398–406 (2013).
3. T. Čižmár and K. Dholakia, "Exploiting multimode waveguides for pure fibre-based imaging," *Nat. Commun.* **3**(1), 1027 (2012).
4. L. G. Wright, D. N. Christodoulides, and F. W. Wise, "Spatiotemporal mode-locking in multimode fiber lasers," *Science* **358**(6359), 94–97 (2017).
5. R. Guenard, K. Krupa, R. Dupiol, M. Fabert, A. Bendahmane, V. Kermene, A. Desfarges-Berthelemot, J. L. Auguste, A. Tonello, A. Barthélémy, G. Millot, S. Wabnitz, and V. Couderc, "Nonlinear beam self-cleaning in a coupled cavity composite laser based on multimode fiber," *Opt. Express* **25**(19), 22219–22227 (2017).
6. M.E. Fernmann and D. J. Harter, "Single-mode amplifier and compressors based on multimode fibers," US Patent 5818630 (1998).
7. K. Krupa, A. Tonello, A. Barthélémy, V. Couderc, B. M. Shalaby, A. Bendahmane, G. Millot, and S. Wabnitz, "Observation of geometric parametric instability induced by the periodic spatial self-imaging of multimode waves," *Phys. Rev. Lett.* **116**(18), 183901 (2016).
8. K. Krupa, A. Tonello, B. M. Shalaby, M. Fabert, A. Barthélémy, G. Millot, S. Wabnitz, and V. Couderc, "Spatial beam self-cleaning in multimode fibres," *Nat. Photonics* **11**(4), 237–241 (2017).
9. Z. Liu, L. G. Wright, D. N. Christodoulides, and F. W. Wise, "Kerr self-cleaning of femtosecond-pulsed beams in graded-index multimode fiber," *Opt. Lett.* **41**(16), 3675–3678 (2016).
10. L. G. Wright, Z. Liu, D. A. Nolan, M.-J. Li, D. N. Christodoulides, and F. W. Wise, "Self-organized instability in graded index multimode fibres," *Nat. Photonics* **10**(12), 771–776 (2016).
11. K. Krupa, A. Tonello, V. Couderc, A. Barthelemy, G. Millot, D. Modotto, and S. Wabnitz, "Spatiotemporal light beam compression from nonlinear mode coupling," *Phys. Rev. A* **97**(4), 043836 (2018).
12. E. Deliancourt, M. Fabert, A. Tonello, K. Krupa, A. Desfarges-Berthelemot, V. Kermene, G. Millot, A. Barthelemy, S. Wabnitz, and V. Couderc, "Kerr beam auto-selection of a low order mode in graded-index multimode fiber," *OSA Continuum* **2**(4), 1089–1096 (2019).
13. E. Deliancourt, M. Fabert, A. Tonello, K. Krupa, A. Desfarges-Berthelemot, V. Kermene, G. Millot, A. Barthelemy, S. Wabnitz, and V. Couderc, "Wavefront shaping for optimized many-mode Kerr beam self-cleaning in graded-index multimode fiber," *Opt. Express* **27**(12), 17311–17321 (2019).
14. E. V. Podivilov, D. S. Kharenko, V. A. Gonta, K. Krupa, O. S. Sidelnikov, S. Turitsyn, M. P. Fedoruk, S. A. Babin, and S. Wabnitz, "Hydrodynamic 2D Turbulence and Spatial Beam Condensation in Multimode Optical Fibers," *Phys. Rev. Lett.* **122**(10), 103902 (2019).
15. A. Fusaro, J. Garnier, K. Krupa, G. Millot, and A. Picozzi, "Dramatic Acceleration of Wave Condensation Mediated by Disorder in Multimode Fibers," *Phys. Rev. Lett.* **122**(12), 123902 (2019).
16. P. Aschieri, G. Garnier, C. Michel, V. Doya, and A. Picozzi, "Condensation and thermalization of classical optical waves in a waveguide," *Phys. Rev. A* **83**(3), 033838 (2011).
Vol. 28, No. 10 / 11 May 2020 / Optics Express 14344
17. J. Garnier, A. Fusaro, K. Baudin, C. Michel, K. Krupa, G. Millot, and A. Picozzi, "Wave condensation with weak disorder versus beam self-cleaning in multimode fibers," *Phys. Rev. A* **100**(5), 053835 (2019).
18. W. H. Renninger and F. W. Wise, "Optical solitons in graded-index multimode fibres," *Nat. Commun.* **4**(1), 1719 (2013).
19. K. Krupa, G. G. Castañeda, A. Tonello, A. Niang, D. S. Kharenko, M. Fabert, V. Couderc, G. Millot, U. Minoni, D. Modotto, and S. Wabnitz, "Nonlinear polarization dynamics of Kerr beam self-cleaning in a graded-index multimode optical fiber," *Opt. Lett.* **44**(1), 171–174 (2019).
20. J. Lægsgaard, "Spatial beam cleanup by pure Kerr processes in multimode fibers," *Opt. Lett.* **43**(11), 2700–2703 (2018).
21. D. Strickland and G. Mourou, "Compression of amplified chirped optical pulses," *Opt. Commun.* **56**(3), 219–221 (1985).
22. Y. Zhang, Y. Cao, and J.-X. Cheng, "High-resolution photoacoustic endoscope through beam self-cleaning in a graded index fiber," *Opt. Lett.* **44**(15), 3841–3844 (2019).

23. U. Tegin, E. Kakkava, B. Rahmani, D. Psaltis, and C. Moser, "Spatiotemporal self-similar fiber laser," *Optica* **6**(11), 1412–1415 (2019).
24. R. Guenard, K. Krupa, R. Dupiol, M. Fabert, A. Bendahmane, V. Kermene, A. Desfarges-Berthelemot, J. L. Auguste, A. Tonello, A. Barthélémy, G. Millot, S. Wabnitz, and V. Couderc, "Kerr self-cleaning of pulsed beam in an ytterbium doped multimode fiber," *Opt. Express* **25**(5), 4783–4792 (2017).

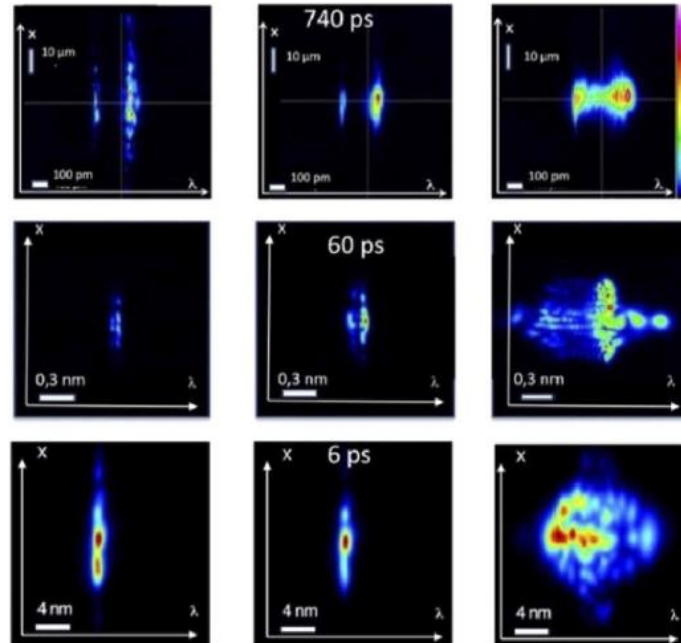


Fig. 1. Spectrograms (intensity vs. transverse coordinate x and wavelength λ) in the near field at the GRIN-MMF output, as a function of the output power (from left to right, 10 W, 1 kW, and 45 kW, respectively) and input pulse width (from top to bottom), 740 ps, 60 ps and 6 ps, respectively, for propagation in the normal dispersion regime (50/125 GRIN-MMF). The ratio between the pulse duration and the differential group-delay in the MMF is: 61, 5 and 1 for the row 1, 2 and 3, respectively.

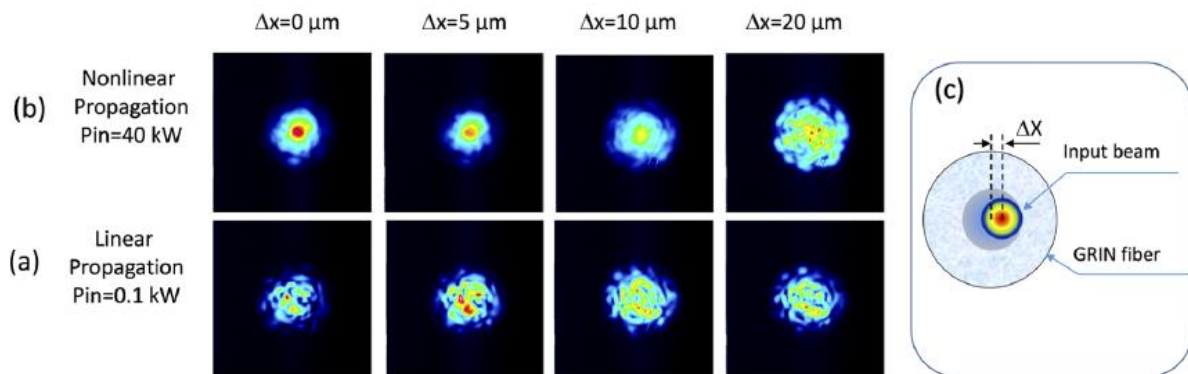


Fig. 2. Output beam intensity patterns versus input beam position with respect to the fiber center. (a) Linear regime, (b) nonlinear regime, (c) scheme of beam coupling (multimode GRIN fiber: 50/125, length: 3 m, input beam diameter: 36 μm - measured at $1/e^2$).

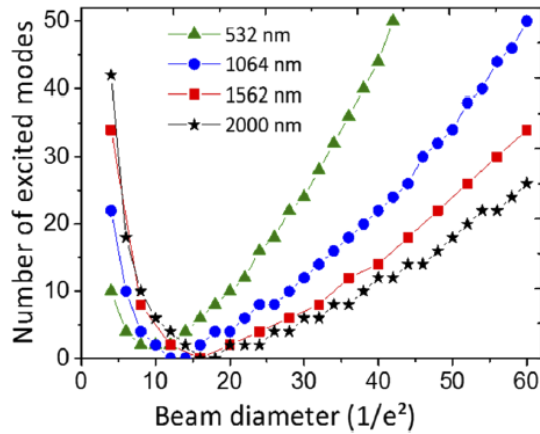


Fig. 3. Number of excited radial scalar modes (with more than 99% of input beam energy) vs. input beam diameter for four different input wavelengths.

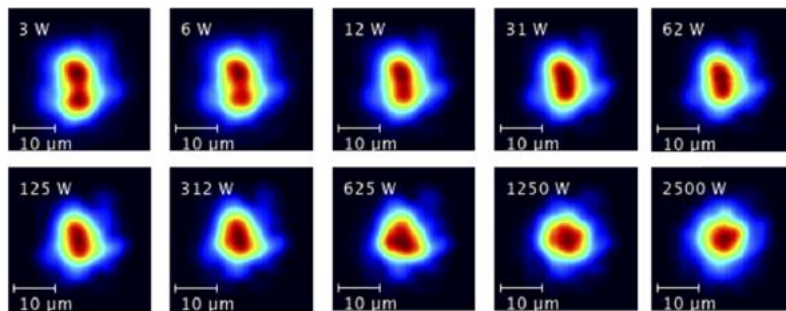


Fig. 4. Near field intensity patterns at the GRIN-MMF output recorded for increasing input peak powers, for appropriate settings of the input coupling, to get the self-selection of a LP₀₁ mode.

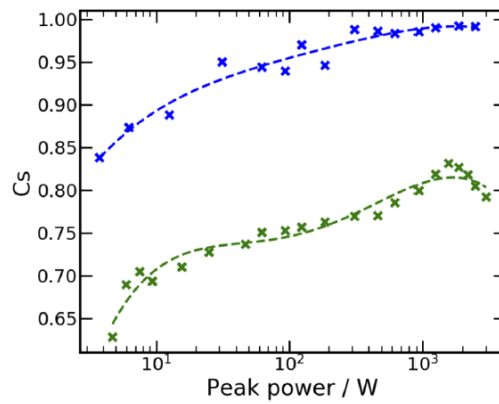


Fig. 5. Intensity correlation Cs upon output peak power for LP₀₁ (blue curve) and LP₁₁ (green curve); dashed lines are guides for the eyes.

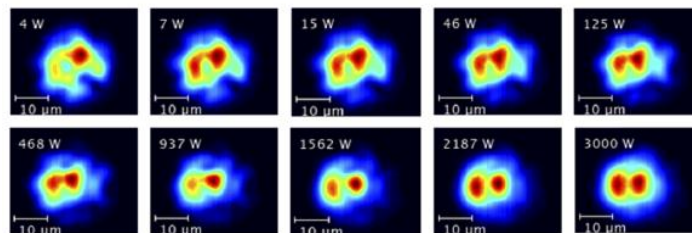


Fig. 6. Near field intensity patterns at the GRIN-MMF output recorded for increasing input peak powers, for appropriate settings of the input coupling, to obtain self-selection of a LP₁₁ mode.

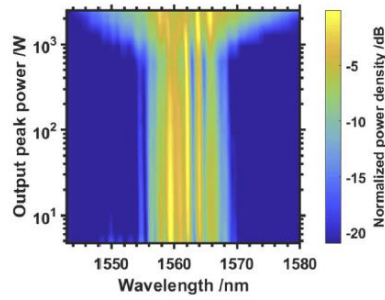


Fig. 7. Experimental power spectral density (normalized to its local peak value) of pulses at the output of the GRIN MMF, as a continuous function of the peak power.

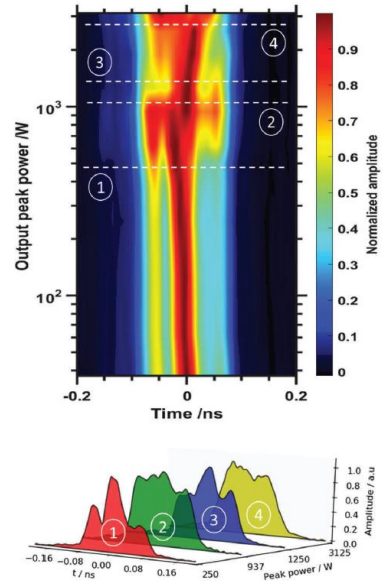


Fig. 8. Top: experimental output temporal profile upon peak power. The horizontal dashed lines represent selected peak power levels, whose corresponding waveforms are plotted in the bottom panel.

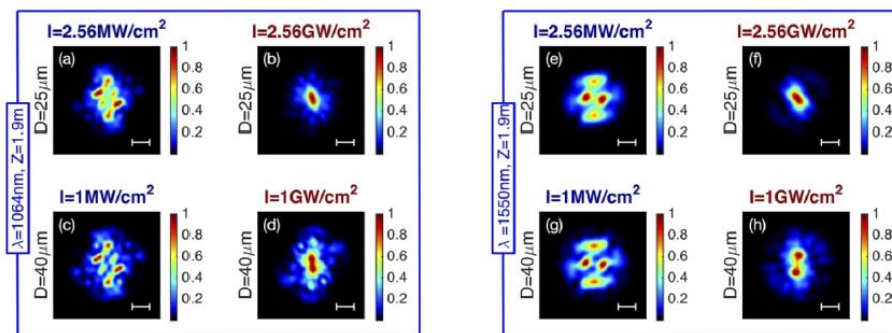


Fig. 9. Numerical simulations of beam reshaping in 1.9 m of GRIN fibers. Panels (a,b,c,d) refer to a central wavelength of 1064 nm and panels (e,f,g,h) refer to the central wavelength of 1550 nm . The white segment indicates 10 μ m.